Cell, Vol. 83, 443–449, November 3, 1995, Copyright © 1995 by Cell Press

Identification of Domains Conferring G Protein Regulation on Inward Rectifier Potassium Channels

Maya T. Kunkel and Ernest G. Peralta
Department of Molecular and Cellular Biology
Harvard University
Cambridge, Massachusetts 02138

Summary

Cardiac m2 muscarinic acetylcholine receptors reduce heart rate by coupling to heterotrimeric (αβγ) guanine nucleotide-binding (G) proteins that activate I_{KACh}, an inward rectifier K^+ channel (IRK). Activation of the GIRK subunit of I_{KACh} requires $G_{\beta\gamma}$ subunits; however, the structural basis of channel regulation is unknown. To determine which sequences confer $G_{\beta\gamma}$ regulation upon IRKs, we generated chimeric proteins composed of GIRK and RB-IRK2, a related, G protein-insensitive channel. Importantly, a chimeric channel containing the hydrophobic pore region of RB-IRK2 joined to the amino and carboxyl termini of GIRK exhibited voltage- and receptor-dependent activation in Xenopus oocytes. Furthermore, carboxy-terminal sequences specific to this chimera and GIRK bound $G_{\beta\gamma}$ subunits in vitro. Thus, $G_{\beta\gamma}$ may regulate IRKs by interacting with sequences adjacent to the putative channel pore.

Introduction

Inward rectifier K^+ channels (IRKs) are widely expressed within the brain and periphery, where they play important roles in controlling the resting membrane potential of excitable and nonexcitable cells. IRKs help set the resting potential of a cell near the K^+ equilibrium potential (E_K) by conducting substantial inward K^+ currents at membrane potentials negative to E_K and small outward currents at voltages positive to E_K (Hille, 1992). Although the gating of IRKs is not restricted to a fixed range of membrane potentials, molecular cloning studies have shown that these channels do share significant structural similarities with the voltage-gated, outwardly rectified K^+ channels (Jan and Jan, 1992). The primary structure of several cloned IRK proteins is proposed to include intracellular amino and carboxyl termini, as well as a hydrophobic domain containing two transmembrane segments (M1 and M2) and a linker region (H5) (Kubo et al., 1993a, 1993b; Ho et al., 1993). Since a similar hydrophobic region present in the voltage-gated K^+ channels has been shown to contribute to the pore structure of these channels, the M1–H5–M2 domain is thought to serve the same function within IRKs (Kubo et al., 1993a).

Although the activation of IRK currents is controlled by the extracellular K^+ concentration and membrane potential, the gating of some channels within this family is also influenced by cytoplasmic factors. One of the most important physiological examples of IRK regulation by an intracellular pathway involves the hormonal stimulation of a cardiac K^+ current termed I_{KACh} (Hille, 1992). Following acetylcholine release from the vagus nerve, m2 muscarinic acetylcholine receptors (mAChRs) expressed on atrial cells activate heterotrimeric (αβγ) guanine nucleotide-binding (G) proteins that in turn stimulate the I_{KACh} channel (Soejima and Noma, 1984; Pfaffinger et al., 1985; Breitweiser and Szabo, 1985). The increased K^+ conductance due to I_{KACh} reduces the rate at which cardiac pacemaker cells depolarize and thus slows heart contraction. Electrophysiological studies have shown that activation of I_{KACh} is a membrane-delimited process that may involve a direct interaction between $G_{\beta\gamma}$ subunits and the channel (Soejima and Noma, 1984; Logothetis et al., 1987; Wickman et al., 1994). Molecular cloning approaches using Xenopus laevis oocytes originally identified the GIRK (Kir3.1) protein as a major component of I_{KACh}, although recent studies indicate that I_{KACh} expressed in heart cells is a heteromultimeric channel composed of GIRK and a second, related protein termed the cardiac inward rectifier (CIR) (Kir3.4) (Kubo et al., 1993b; Dascal et al., 1993; Krapivinsky et al., 1995). Initial experiments with GIRK and CIR support the notion that $G_{\beta\gamma}$ subunits activate I_{KACh}; however, little is known about the structural basis of IRK regulation by G proteins (Reuveny et al., 1994; Krapivinsky et al., 1995).

By constructing chimeric proteins composed of GIRK and a related but G protein–insensitive inward rectifier termed RB-IRK2 (Kir2.2), we have identified particular channel domains that are important for voltage-dependent or G protein–activated inward K^+ currents. In addition, we conducted experiments that tested whether specific GIRK domains can directly bind $G_{\beta\gamma}$ subunits. These in vivo and in vitro studies indicate that $G_{\beta\gamma}$ subunits may regulate IRKs by interacting with intracellular domains adjacent to the hydrophobic channel pore region.

Results

Regulation of GIRK, RB-IRK2, and Chimeric Channels

Primary sequence conservation between the GIRK and RB-IRK2 channels is greatest within the putative pore (M1–H5–M2) domain and first half of the carboxy-terminal (C1) region, where these proteins are 47% and 58% identical, respectively (Figure 1). The amino termini (N) of GIRK and RB-IRK2 share 37% of their residues in common, whereas the remaining carboxy-terminal region (C2) of RB-IRK2 is 73 amino acids shorter than GIRK and exhibits very little sequence similarity (Figure 1). Previous studies have shown that the RB-IRK2 channel conducts inward currents in RNA-injected Xenopus oocytes when the membrane potential is held negative to E_K (Koyama et al., 1994). In contrast, activation of inward GIRK currents requires membrane hyperpolarization as well as a $G_{\beta\gamma}$ subunit-dependent signal (Kubo et al., 1993b; Reuveny et al., 1994).

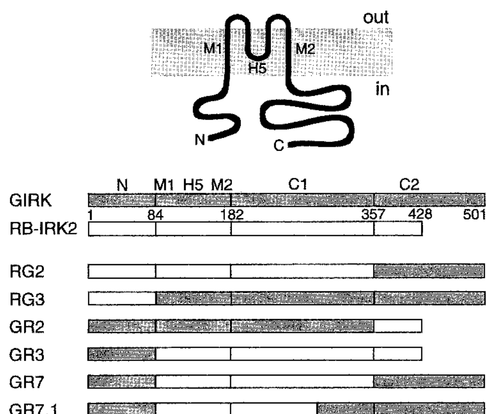

Figure 1. Structure of Wild-Type and Chimeric Channels

Top, the proposed topology of IRK channels. The numbering refers to the amino acid boundaries of each domain; GIRK domains are shaded. The N, M1–H5–M2, and C1 domains of GIRK and RB-IRK2 share 37%, 47%, and 58% of their amino acids in common, respectively. The C2 domain of RB-IRK2 is 73 amino acids shorter than the corresponding region of GIRK and shares little similarity. The C1 domain of chimera GR7.1 contains amino acids 182–289 of RB-IRK2 joined to amino acids 290–356 of GIRK.

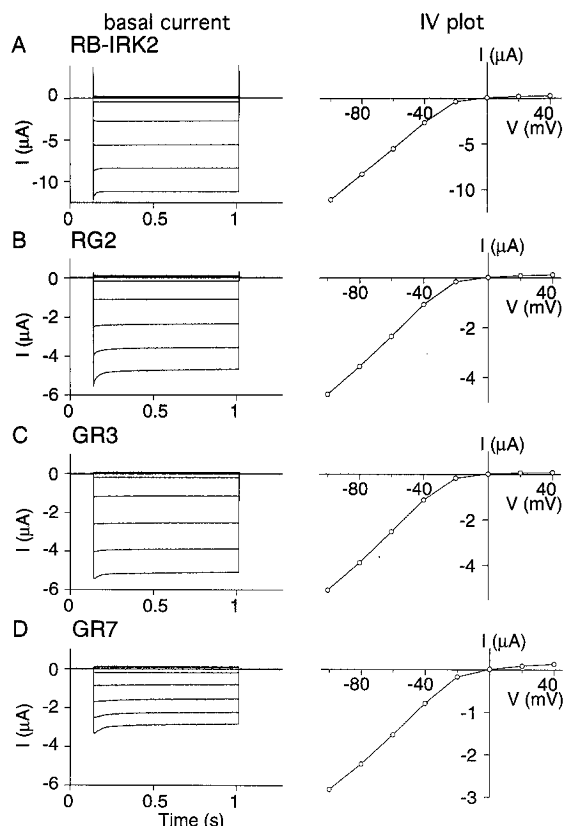

Figure 2. Functional Expression of RB-IRK2 and IRK Chimeras

Representative traces of voltage-dependent (basal) currents obtained from oocytes expressing RB-IRK2 (A), RG2 (B), GR3 (C), and GR7 (D) channels are shown. Oocytes were injected with in vitro transcribed RNAs encoding the m2 mAChR, G protein subunits α_{i3}, β_1, and γ_2, and the indicated channels. Because the RB-IRK2, GR3, and RG2 currents were typically 10-fold larger (20–80 μA) than those displayed by GR7, only 1 ng of these transcripts was injected, versus 10 ng of GR7 RNA, to produce whole-cell currents less than 15 μA. Cells were recorded in high (90 mM) K^+ saline resulting in a predicted K^+ reversal potential of 0 mV. I–V plots were obtained from the steady-state currents of the basal, nonsubtracted traces shown at left. RB-IRK2, RG2, GR3, and GR7 currents were not affected by activation of the m2 mAChR with 10 μM carbachol.

To measure voltage- and G protein–induced currents generated by wild-type and chimeric IRKs, we injected Xenopus oocytes with RNAs encoding the channel protein, m2 mAChR, $G_{\alpha i3}$, $G_{\beta 1}$, and $G_{\gamma 2}$. Whole-cell currents were measured in a 90 mM extracellular K^+ recording solution; under these conditions, the predicted reversal potential for a K^+-selective current is 0 mV. Oocytes injected with RNA encoding RB-IRK2 displayed large, inward whole-cell currents that reached a maximum amplitude at the start of each voltage pulse (Figure 2A). Furthermore, RB-IRK2 currents were unaltered following activation of the m2 mAChR with 10 μM carbachol (data not shown). In contrast, small inward currents were detected in GIRK-expressing oocytes only after the m2 mAChR was stimulated with carbachol. Analysis of the carbachol-induced current, obtained by subtracting the precarbachol current traces from the postcarbachol traces, revealed the slow rate at which GIRK currents reached their maximum amplitude during each voltage pulse (see Figure 3A) (Kubo et al., 1993b). As expected for a direct G protein activation mechanism, the onset of GIRK currents occurred in less than 1 s (0.8 ± 0.1 s, $n = 12$) after agonist application. Therefore, the carbachol dependence and relatively slow gating of GIRK currents readily distinguished the responses of this channel from those of the structurally related RB-IRK2.

We constructed a variety of chimeras based on the putative four domain structure (N/M1–H5–M2/C1/C2) shown in Figure 1, although many of these failed to generate functional channels (see Experimental Procedures). Several chimeric channels were expressed in oocytes and characterized by their ability to generate ionic currents in response to changes in membrane potential and agonist activation of the m2 mAChR. Transfer of either the N or C2 domain of GIRK into the corresponding region of RB-IRK2 resulted in two chimeric proteins, GR3 and RG2, respectively, that evoked robust, inwardly rectifying K^+ currents when the membrane potential was held negative to E_K (Figures 2B and 2C). The magnitude and kinetics of GR3 and RG2 currents closely resembled the responses recorded from RB-IRK2-injected oocytes; moreover, the currents generated by both chimeras were unaffected by the addition of carbachol (data not shown). When both the N and C2 regions of GIRK were exchanged for the corresponding sequences of RB-IRK2, the resulting chimeric channel, termed GR7, activated rapidly in response to membrane hyperpolarization, but produced whole-cell currents of much smaller magnitude than those of RB-IRK2, GR3, or RG2 (Figure 2). These relatively small whole-cell currents may reflect a property of individual

GR7 channels or lower levels of expression compared with those of other channel proteins. As with chimeras GR3 and RG2, the currents generated by GR7 were not altered by agonist stimulation of the m2 mAChR (see below).

Exchange of the carboxy-terminal C2 region of RB-IRK2 into GIRK resulted in a chimeric channel, termed GR2, that did not exhibit IRK activity when the membrane potential was held at hyperpolarized potentials. However, immediately following the application of carbachol, GR2-expressing oocytes displayed inwardly rectified currents that were similar in kinetics, yet much smaller in magnitude, than those conducted by the GIRK channel (Figure 3C). GIRK-based chimeras containing the N, M1–H5–M2, or C1 regions derived from RB-IRK2 did not produce voltage or carbachol-activated channels in RNA-injected oocytes. We also constructed deletion mutants of GIRK to test the importance of sequences within the N domain that are poorly conserved with RB-IRK2. Oocytes expressing GIRK deletion mutants lacking a hydrophilic-rich (residues 5–24) or glutamine- and proline-rich (residues 25–36) region generated carbachol-dependent inward currents that were identical to those of the wild-type GIRK channel (data not shown). Together with analysis of the GR2 chimera, these results indicate that approximately half of the N domain (residues 5–36) and the entire carboxy-terminal C2 region are not specifically required for the G protein–dependent activation of GIRK.

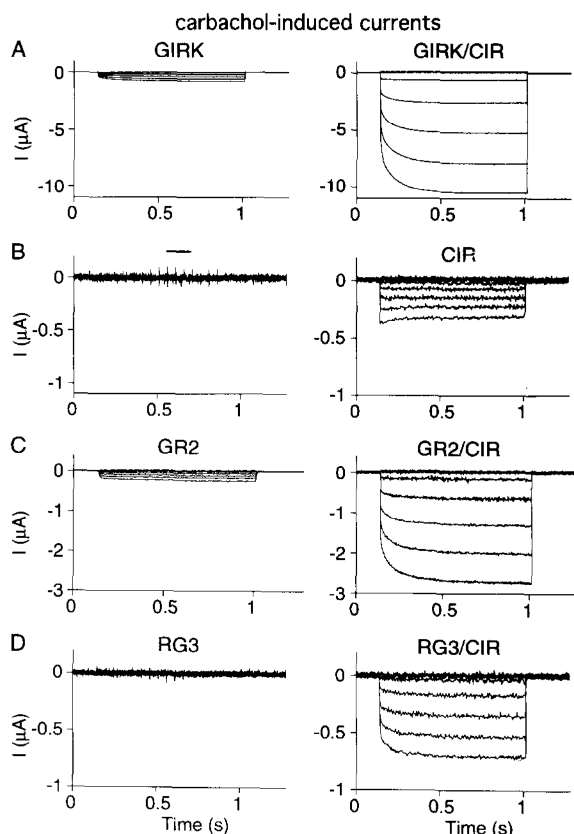

Figure 3. Coexpression with CIR Enhances m2 mAChR–Dependent Activation of GIRK and Chimeras Containing the Central Domains of GIRK

Oocytes were injected with transcripts encoding the m2 mAChR, $G_{\alpha\beta\gamma}$, and either GIRK (A), no channel (B), GR2 (C), or RG3 (D), with (right) and without (left) CIR. Representative traces are shown of the carbachol-induced currents obtained by subtraction of precarbachol traces from postcarbachol traces. Similar results were obtained from six or more oocytes per experiment.

Coexpression of IRKs and CIR

Recent functional analysis of cloned IRKs indicates that the native I_{KACh} channel is a heteromultimer composed of GIRK and the related CIR protein (Krapivinsky et al., 1995). Therefore, we determined whether CIR could influence the characteristics of the wild-type and chimeric IRKs utilized in our study. Oocytes injected with CIR transcripts alone displayed voltage-dependent IRK activity only after activation of the m2 mAChR with carbachol; these currents presumably arise from homomeric CIR channels (Figure 3B). As previously reported, coexpression of GIRK and CIR resulted in a substantial (10- to 15-fold) increase in the amplitude of carbachol-induced currents (Figure 3A) (Krapivinsky et al., 1995). However, oocytes that were coinjected with CIR and RB-IRK2 transcripts generated currents that were greatly reduced compared with the responses recorded from oocytes expressing RB-IRK2 alone (data not shown). Activation of the m2 mAChR evoked a small increase in the inward currents recorded in oocytes coinjected with RB-IRK2 and CIR transcripts; however, these currents were identical in magnitude to the responses recorded in oocytes expressing CIR alone. These results suggest that heteromultimerization with CIR selectively enhances the amplitude of GIRK, but not RB-IRK2, currents.

We coinjected oocytes with RNAs encoding CIR and each of the chimeras, including those that failed to exhibit voltage or G protein–activated currents when expressed on their own. Similar to the effect on the wild-type GIRK channel, coexpression of CIR with chimera GR2 caused a substantial (10- to 15-fold) increase in the amplitude of m2 mAChR–induced currents without changing the kinetics or carbachol dependence of these responses (Figure 3C). Among the several chimeric proteins that failed previously to exhibit channel activity, only chimera RG3, a GIRK-based protein in which only the N domain was derived from RB-IRK2 (see Figure 1), displayed channel activity as a result of coexpression with CIR. Oocytes injected with both RG3 and CIR transcripts exhibited carbachol-dependent inward currents of smaller magnitude but kinetics similar to those recorded in oocytes that coexpressed CIR with either GIRK or GR2 (Figure 3D). The GIRK-like responses generated by putative RG3–CIR heteromultimers further suggests that the N domain of GIRK is not specifically required for channel activation by G proteins.

Receptor Activation of Chimera GR7.1

Since the GR7 chimera contained the hydrophobic pore and C1 domains derived from RB-IRK2 and exhibited only the functional characteristics of this channel, we constructed related chimeras to determine whether the introduction of additional GIRK sequences within the con-

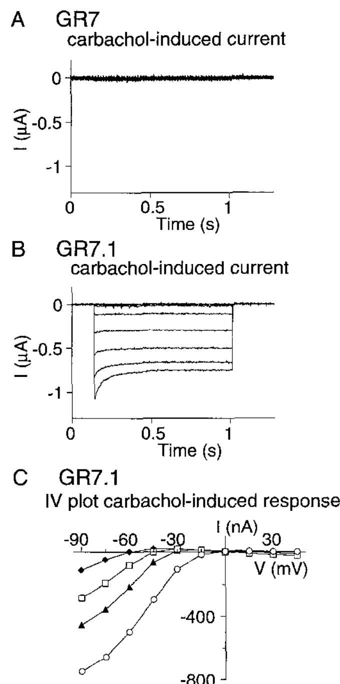

Figure 4. Chimera GR7.1 Exhibits Basal and m2 mAChR Enhanced Inward K^+ Currents

Carbachol-induced currents obtained as in Figure 3 are shown from oocytes injected with transcripts encoding the m2 mAChR, $G_{\alpha\beta\gamma}$, and GR7 (A) or GR7.1 (B).

(A) m2 mAChR activation by 10 μM carbachol had no effect on basal GR7 currents (3% ± 1% carbachol-induced increase, n = 10). The GR7-expressing cell was held at 0 mV in 90 mM K^+ saline and stepped from +40 to −100 mV in 20 mV increments.

(B) Activation of the m2 mAChR with 10 mM carbachol enhanced the inwardly rectified K^+ current in GR7.1-expressing oocytes (42% ± 5% carbachol-induced increase, n = 16). Representative traces obtained in 90 mM K^+ saline are shown. The GR7.1 oocyte was held at 0 mV and pulsed from +45 to −90 mV in 15 mV increments.

(C) The I-V relationship of the carbachol-enhanced GR7.1 currents was obtained by repeating the voltage protocol on the same oocyte before and after m2 mAChR activation in the following K^+ concentrations: open circles, 90 mM; closed triangles, 45 mM; open squares, 22.5 mM; and closed diamonds, 11.25 mM with Na^+ substituted for K^+.

served C1 region could confer G protein regulation upon the resulting channels. One such chimera, designated GR7.1, contained the N, C2, and carboxy-terminal 67 residues of the C1 region derived from GIRK (see Figure 1). This chimera exhibited voltage-dependent K^+ currents of a magnitude similar to those recorded in oocytes expressing GR7. However, unlike the parental GR7 chimera, the basal inward K^+ currents conducted by GR7.1 channels were enhanced immediately after activation of the m2 mAChR (Figure 4). The amplitude of whole-cell GR7.1 currents recorded at −100 mV increased by 42% ± 5% (n = 16) following carbachol addition, while GR7 currents were essentially unaffected by m2 mAChR signaling (3% ± 1% increase, n = 10) (Figure 4). The reversal potential of the carbachol-induced GR7.1 current shifted with changes in the external K^+ concentration in agreement with the Nernst equation for a K^+-selective conductance (Figure 4C). In addition, the basal and carbachol-induced current was blocked by the external application of the K^+ channel blocker barium (100 μM final concentration; data not shown). The onset of GR7.1 current enhancement occurred in less than 1 s (0.7 ± 0.1 s, n = 10) after carbachol addition and thus resembled the time course of GIRK activation by the m2 mAChR (0.8 ± 0.1 s, n = 12). Oocytes coinjected with CIR and GR7 or GR7.1 transcripts failed to produce significant voltage-dependent IRK currents, although carbachol did evoke small inward currents of a magnitude comparable to those recorded in oocytes expressing CIR alone (data not shown). Thus, unlike the G protein–activated GIRK, RG3, and GR2 channels, the magnitude of carbachol-stimulated GR7.1 currents was not enhanced by coexpression with CIR.

$G_{\beta\gamma}$ Binding to IRK Cytoplasmic Domains

Previous electrophysiological studies suggest that activation of I_{KACh} by $G_{\beta\gamma}$ subunits may involve a direct interaction between the channel and G protein (Wickman et al., 1994; Reuveny et al., 1994). To investigate this possibility further, we expressed the domains of GIRK flanking the hydrophobic pore region as glutathione S-transferase (GST) fusion proteins (GIRK-N, GIRK-C1, GIRK-C2) and tested for their ability to bind $G_{\beta\gamma}$. As controls, we also tested the GST protein alone or GST fused to the β-adrenergic receptor kinase pleckstrin homology domain (βARK-PH), a known $G_{\beta\gamma}$-binding protein (Koch et al., 1994). Each GST fusion protein was purified from bacteria by immobilization on glutathione-conjugated agarose beads and incubated with total cell extracts derived from 293 cells that were transiently transfected with plasmids encoding murine $G_{\beta 1}$ and $G_{\gamma 2}$ (Tsukada et al., 1994). Following washing, proteins bound to the agarose beads were released by boiling and analyzed by immunoblotting with a $G_{\beta 1}$-specific antisera. Interestingly, we observed $G_{\beta 1}$ protein binding to both the N and the C1 regions of GIRK, as well as the positive control βARK-PH domain, but not to the GIRK C2 region or GST alone (Figure 5A). These results are consistent with the possibility that $G_{\beta\gamma}$ subunits activate GIRK by interacting directly with the C1 and N regions.

Functional analysis of the GR7 and GR7.1 chimeras revealed that while both channel proteins displayed voltage-dependent IRK activity, only GR7.1 currents were enhanced by signaling through the m2 mAChR (see Figure 4). These two chimeras differ only within the C1 domain: this region of GR7 is composed entirely of RB-IRK2 sequences, while the GR7.1 contains 67 residues derived from GIRK (see Figure 1). Therefore, to investigate whether activation of a wild-type or chimeric IRK channel by the m2 mAChR correlated with the capacity of the C1 region to interact with $G_{\beta\gamma}$ subunits, we analyzed GST fusion proteins containing the C1 domain of GIRK, RB-IRK2, and GR7.1 by using the in vitro binding assay described above. Interestingly, the C1 region of GIRK and GR7.1 displayed equivalent $G_{\beta\gamma}$ binding as detected by immunoblotting with the $G_{\beta 1}$-specific antisera (Figure 5B). In contrast, the C1 region of RB-IRK2 did not interact significantly with $G_{\beta\gamma}$ subunits. Therefore, the GR7.1 chimera not only

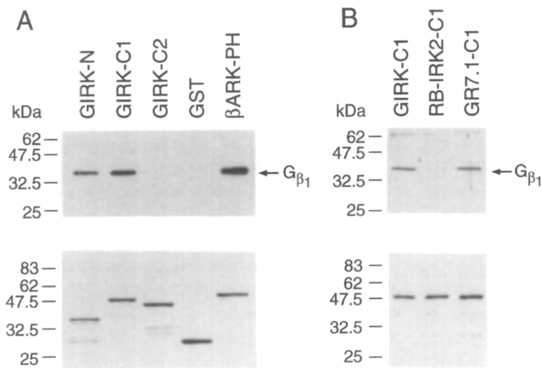

Figure 5. In Vitro $G_{\beta\gamma}$ Binding to IRK Domains

(A) Immunoblot of $G_{\beta\gamma}$ binding to GST fusion proteins. The boundaries of each IRK domain are described in Figure 1. Purified GST proteins immobilized on glutathione-conjugated agarose beads were incubated with a crude cell lysate derived from 293 cells that were transiently transfected with expression vectors encoding $G_{\beta 1}$ and $G_{\gamma 2}$. After washing, proteins bound to beads were released by boiling and separated by SDS–PAGE. $G_{\beta 1}$ protein was detected by immunoblotting with anti-β1 antisera (top), and GST fusion proteins were detected by Coomassie staining (bottom).

(B) $G_{\beta 1\gamma 2}$ associates with the C1 domain from both GIRK and GR7.1, but to a much lesser extent with the C1 domain of RB-IRK2. The assay was performed as described in (A). Results shown in (A) and (B) were repeated in two or more independent experiments.

exhibited carbachol-stimulated inward K^+ currents, but also shared with GIRK the ability to bind $G_{\beta\gamma}$ subunits via the carboxy-terminal C1 region of the channel.

Discussion

IRKs can modulate cell excitability by determining the ease with which depolarizing currents reach the threshold necessary to evoke an action potential (Hille, 1992). Therefore, regulation of IRKs by G protein–coupled receptors constitutes an important mechanism by which neurotransmitters influence the electrophysiological activity of many cell types. However, very little is known about the structural basis of IRK regulation by G proteins or other intracellular signaling molecules.

By analyzing a series of chimeric channel proteins, we found that the hydrophobic pore (M1–H5–M2) and adjacent C1 regions largely determine the regulatory properties of both RB-IRK2 and GIRK. The GR3, RG2, and GR7 chimeras displayed rapidly gated, voltage-dependent currents characteristic of RB-IRK2, even though these channels contained either or both of the N and C2 regions derived from GIRK, respectively (Figure 1). In addition, the channel activity of these three chimeras was not increased by signaling through the m2 mAChR or coexpression with the CIR subunit. The RG3 and GR2 chimeras, which contained the pore and C1 regions of GIRK joined to the N or C2 regions of RB-IRK2, respectively, exhibited IRK activity only after stimulation of the m2 mAChR with carbachol. The magnitude of the carbachol-induced GR2 current was increased by coexpression with CIR, while the GIRK-like responses of the RG3 chimera were completely dependent upon CIR. The stimulatory effect of CIR on GR2 and RG3 channel activity suggests that productive multimerization with CIR does not require sequences unique to the N or C2 domains of GIRK. Therefore, the domains that are least conserved between RB-IRK2 and GIRK, namely the N and C2 regions, do not include the structural information that specifies voltage and G protein–dependent channel activation or the gating kinetics of these two IRKs. Instead, the relatively well-conserved pore and C1 regions appear to contain the major determinants of these properties. Although the pore and C1 regions may play a dominant role in the regulation of IRKs by $G_{\beta\gamma}$, we have not been able to generate a functioning channel that lacks the entire N or C2 region (unpublished data). Similarly, others have found that deletion of the carboxy-terminal 146 amino acids of GIRK (i.e., C2) abolished channel activity (Reuveny et al., 1994). Thus, the N and C2 regions may be required for certain RB-IRK2 or GIRK functions, but this requirement may be met by sequences derived from either channel.

Analysis of the GR7 and GR7.1 channels demonstrated that sequences within the carboxyl terminus of the GIRK C1 region are particularly important for the regulation of channel activity by the m2 mAChR. Unlike the GR7 chimera, carbachol caused an immediate and substantial (~40%) increase in the whole-cell K^+ currents produced by the GR7.1 channel. The onset of GR7.1 current enhancement was less than 1 s after carbachol addition and therefore identical to the time course of GIRK activation. Since these two chimeras vary in only 27 of the 67 residues within the carboxy-terminal portion of the C1 domain, relatively small sequence differences within this region can determine the sensitivity of a channel to m2 mAChR signaling. However, a chimera containing only the carboxy-terminal C1 region of GIRK within RB-IRK2 displays voltage-dependent IRK currents that are not enhanced by the m2 mAChR (unpublished data). Therefore, sequences within the C1 region may interact with other GIRK-specific residues to mediate m2 mAChR–dependent regulation of chimeric or wild-type GIRK channels.

Previous studies have shown that activation of I_{KACh} or GIRK by the m2 mAChR is mediated by $G_{\beta\gamma}$ subunits, although it is unknown whether $G_{\beta\gamma}$ interacts directly with the channel or through an associated protein (Logothetis et al., 1987; Reuveny et al., 1994; Wickman et al., 1994). We found that purified bacterial fusion proteins containing either the N or C1, but not the C2, regions of GIRK were capable of binding $G_{\beta\gamma}$ subunits present in mammalian cell lysates. More importantly, the ability of a C1 fusion protein to bind $G_{\beta\gamma}$ subunits in vitro correlated with the capacity of the corresponding wild-type or chimeric channel to be activated by the m2 mAChR in vivo. Reuveny and colleagues (1994) have noted that sequences within the carboxyl terminus of GIRK are weakly related to the PH domain of βARK. However, the critical portion of the C1 region defined by our study shares little similarity with this PH domain or to the novel $G_{\beta\gamma}$ regulatory region in adenylyl cyclase 2 (Chen et al., 1995). Further mapping studies will be required to determine whether this region of GIRK

defines a new $G_{\beta\gamma}$-binding motif. It is interesting to note that the carboxyl terminus of the ATP-sensitive ROMK channel contains a consensus nucleotide-binding motif, and that cyclic nucleotide and Ca^{2+}-dependent cation channels also contain binding sites for their activating ligands within the large cytoplasmic carboxyl terminus of each channel (Ho et al., 1993; Goulding et al., 1994; Wei et al., 1994). Therefore, like the outwardly rectifying cation channels, IRKs may have evolved distinct carboxy-terminal binding domains that confer regulation by G protein subunits or other signaling molecules.

Future studies will investigate the mechanism of GR7.1 channel activation by both voltage and m2 mAChR–dependent signals. It is possible that the m2 mAChR–induced increase in GR7.1 currents involves a second messenger pathway rather than a direct G protein mode of channel regulation. However, activation of I_{KACh} by the m2 mAChR does not involve a soluble second messenger (Soejima and Noma, 1984), and the parental RB-IRK2 channel is unaffected by m2 mAChR signaling. Our previous studies also indicate that the time course of K^+ channel modulation by second messenger pathways in Xenopus oocytes is substantially slower than we observed here (Huang et al., 1993, 1994). The extremely rapid onset of carbachol-enhanced GR7.1 currents and the $G_{\beta\gamma}$-binding activity displayed by the C1 domain of this chimera suggest important functional similarities in the mechanism by which the GR7.1 and GIRK channels are activated by the m2 mAChR. We speculate that GIRK-derived sequences within the cytoplasmic domains may interact with the pore region of GR7.1 to inhibit or reduce the magnitude of voltage-dependent channel activity; within the wild-type GIRK protein, these interactions may result in a more complete block of basal channel activity. The m2 mAChR–induced enhancement of whole-cell GR7.1 currents, or activation of GIRK, may reflect the loss of channel inhibition caused by the direct association of $G_{\beta\gamma}$ subunits with the C1 and N domains of the channel. We will investigate these possibilities by analyzing the effect of G proteins on the activation of single GR7.1 and GIRK channels.

Experimental Procedures

Chimeric Channel Construction

Clones encoding GIRK, CIR, and RB-IRK2 were isolated from rat heart cDNA and correspond to the channels reported by Kubo et al. (1993b) (GenBank accession number L25264), Krapivinsky et al. (1995) (GenBank accession number L35771), and Koyama et al. (1994) (GenBank accession number X78461), respectively. All possible chimeras based on the four-part structure depicted in Figure 1 were constructed by polymerase chain reaction (PCR) as described (Lechleiter et al., 1990); only the chimeras shown exhibited channel activity. The amino acid boundaries of the channel domains are as follows: GIRK-N and RB-IRK2-N, 1–83; GIRK-M1–H5–M2 and RB-IRK2-M1–H5–M2, 84–181; GIRK-C1, 182–356; RB-IRK2-C1, 182–357; GIRK-C2, 357–501; and RB-IRK2-C2, 358–427. To construct GR7.1, an XhoI site was introduced into GIRK at nucleic acid residue 862; an XhoI site exists at the equivalent position in RB-IRK2 and, consequently, in chimera GR7. DNA encoding amino acids 290–501 of GIRK (beginning at the XhoI site) was subcloned in place of the sequences encoding the 213 carboxy-terminal amino acids of chimera GR7 to construct GR7.1. Deletion mutants of GIRK were constructed as described (Kunkel and Peralta, 1993). All constructs were confirmed by dideoxynucleotide sequencing.

Oocyte Electrophysiology

RNAs were synthesized and Xenopus laevis oocytes were prepared as described (Kunkel and Peralta, 1993). All oocytes were injected with a 50 nl bolus containing approximately 2 ng of $G_{\alpha i3}$ and $G_{\beta 1}$ RNA, 0.8 ng of $G_{\gamma 2}$ RNA, 3 ng of m2 mAChR RNA, and 10 ng of channel RNA or 1 ng of RB-IRK2, GR3, or RG2 RNA. In coexpression experiments with CIR, equivalent amounts (5 ng) of the transcripts encoding CIR and the wild-type or chimera channel were included in the injection bolus. Under these conditions, we observed consistent m2 mAChR–dependent activation of GIRK currents without generation of a Ca^{2+}-activated Cl^- current. We did not observe basal activation of GIRK except in a subset of oocytes expressing both GIRK and CIR. Oocytes were recorded 3–5 days after injection.

Two-electrode voltage clamp was used to measure whole-cell currents (Kunkel and Peralta, 1993). Electrodes were pulled to a resistance of 0.2–1.0 MΩ and filled with 3 M KCl. Recordings were made at 22°C from oocytes in high K^+ saline (90 mM KCl, 3 mM $MgCl_2$, 5 mM HEPES [pH 7.4]). Oocytes were held at 0 mV and stepped from +40 to −100 mV in 20 mV increments except in the ion substitution experiments of chimera GR7.1, in which the oocytes were held at 0 mV and stepped from +45 to −90 mV in 15 mV increments; the protocol was repeated on the same oocyte before and after carbachol addition in 90 mM, 45 mM, 22.5 mM, and 11.25 mM K^+ saline in which Na^+ was substituted for K^+. In all voltage step experiments, postcarbachol recordings were made immediately after bath addition of 10 μM carbachol. The time to GIRK or GR7.1 current onset due to activation of the m2 mAChR was determined by continuous recording of the whole-cell current at −80 mV while carbachol was manually applied to the bath. Agonist was added and mixed by replacement of one third of the bath volume with saline containing carbachol. Current records were stored and analyzed with pCLAMP version 5.6 and Axograph version 2.0 (Axon Instruments, Foster City, CA).

$G_{\beta\gamma}$ Binding

DNA encoding the N, C1, or C2 regions of wild-type or chimeric channels and βARK-PH domain (amino acids 495–689; Koch et al., 1994) was generated by PCR and fused in-frame to the GST coding sequence in pGEX-2T. Fusion proteins were expressed in Escherichia coli BL21 (DE3) pLysS, induced with 0.5 mM IPTG, and prepared according to the method described by Grieco et al. (1992). The solubilized fusion proteins were purified by incubation with glutathione-conjugated agarose beads at room temperature for 2–5 min and washed three times with 200 vol of PBS, 1% Triton X-100. Approximately 5 μg of GST fusion protein bound to agarose beads was used in each binding assay.

The cDNAs encoding $G_{\beta 1}$ and $G_{\gamma 2}$ were cloned into pcDNA3 (Invitrogen) and transfected into 293 cells by using calcium phosphate, and total cell lysates were prepared and dialyzed against PBS with 0.01% lubrol as described (Tsukada et al., 1994). Purified fusion protein bound to glutathione-conjugated agarose beads was incubated with the 293 cell lysate for 1 hr at 4°C and subsequently washed three times with 200 vol of PBS, 0.01% lubrol as described (Tsukada et al., 1994). Bound proteins were eluted from the beads by heating in protein sample buffer at 100°C and then separated by SDS–PAGE. GST fusion proteins were visualized by Coomassie staining, and $G_{\beta 1}$ protein was detected by immunoblotting using a $G_{\beta 1}$ rabbit polyclonal antibody (BN-1) and visualized with an enhanced chemiluminescence kit (Amersham).

Acknowledgments

We thank Dr. N. Gautam for the $G_{\beta 1}$ and $G_{\gamma 2}$ cDNA clones and anti-$G_{\beta 1}$ antibodies, Dr. R. Lefkowitz for the βARK-PH mini-gene, Dr. A. Morielli for advice with voltage clamp experiments, and D. Garsin for assistance with the early $G_{\beta\gamma}$ binding studies. We thank our lab colleagues for helpful comments during the course of this work. M. T. K. was supported by a predoctoral training grant from the National Institutes of Health. This research was supported by grants to E. G. P. from the National Institutes of Health, the National Science Foundation Presidential Young Investigator Program, and the McKnight Foundation for Neuroscience.

Received July 20, 1995; revised August 31, 1995.

References

Breitweiser, G.E., and Szabo, G. (1985). Uncoupling of cardiac muscarinic and β-adrenergic receptors from ion channels by a guanine nucleotide analogue. Nature *317*, 538–540.

Chen, J., DeVivo, M., Dingus, J., Harry, A., Li, J., Sui, J., Carty, D.J., Blank, J.L., Exton, J.H., Stoffel, R.H., Inglese, J., Lefkowitz, R.J., Logothetis, D.E., Hildebrandt, J.D., and Iyengar, R. (1995). A region of adenylyl cyclase 2 critical for regulation by G protein βγ subunits. Science *268*, 1166–1169.

Dascal, N., Schreibmayer, W., Lim, N.F., Wang, W., Chavkin, C., DiMagno, L., Labarca, C., Kieffer, B.L., Gaveriaux-Ruff, C., Trollinger, D., Lester, H.A., and Davidson, N. (1993). Atrial G protein–activated K+ channel: expression cloning and molecular properties. Proc. Natl. Acad. Sci. USA *90*, 10235–10239.

Goulding, E.H., Tibbs, G.R., and Siegelbaum, S.A. (1994). Molecular mechanism of cyclic-nucleotide-gated channel activation. Nature *372*, 369–374.

Grieco, F., Hay, J.M., and Hull, R. (1992). An improved procedure for the purification of protein fused with glutathione S-transferase. BioTechniques *13*, 856–858.

Hille, B. (1992). Ionic Channels of Excitable Membranes (Sunderland, Massachusetts: Sinauer Associates).

Ho, K., Nichols, C.G., Lederer, W.J., Lytton, J., Vassilev, P.M., Kanazirska, M.V., and Hebert, S.C. (1993). Cloning and expression of an inwardly rectifying ATP-regulated potassium channel. Nature *362*, 31–38.

Huang, X.-Y., Morielli, A.D., and Peralta, E.G. (1993). Tyrosine kinase–dependent suppression of a potassium channel by the G protein–coupled m1 muscarinic acetylcholine receptor. Cell *75*, 1145–1156.

Huang, X.-Y., Morielli, A.D., and Peralta, E.G. (1994). Molecular basis of cardiac potassium channel stimulation by protein kinase A. Proc. Natl. Acad. Sci. USA *91*, 624–628.

Jan, L.Y., and Jan, Y.N. (1992). Structural elements involved in specific K+ channel functions. Annu. Rev. Physiol. *54*, 537–555.

Koch, W.J., Hawes, B.E., Inglese, J., Luttrell, L.M., and Lefkowitz, R.J. (1994). Cellular expression of the carboxyl terminus of a G protein–coupled receptor kinase attenuates $G_{\beta\gamma}$-mediated signaling. J. Biol. Chem. *269*, 6193–6197.

Koyama, H., Morishige, K.-I., Takahashi, N., Zanelli, J.S., Fass, D.N., and Kurachi, Y. (1994). Molecular cloning, functional expression and localization of a novel inward rectifier potassium channel in the rat brain. FEBS Lett. *341*, 303–307.

Krapivinsky, G., Gordon, E.A., Wickman, K., Velimirovic, B., Krapivinsky, L., and Clapham, D.E. (1995). The G-protein-gated atrial K+ channel I_{KACh} is a heteromultimer of two inwardly rectifying K+-channel proteins. Nature *374*, 135–141.

Kubo, Y., Baldwin, T.J., Jan, Y.N., and Jan, L.Y. (1993a). Primary structure and functional expression of a mouse inward rectifier potassium channel. Nature *362*, 127–133.

Kubo, Y., Reuveny, E., Slesinger, P.A., Jan, Y.N., and Jan, L.Y. (1993b). Primary structure and functional expression of a rat G-protein-coupled muscarinic potassium channel. Nature *364*, 802–806.

Kunkel, M.T., and Peralta, E.G. (1993). Charged amino acids required for signal transduction by the m3 muscarinic acetylcholine receptor. EMBO J. *12*, 3809–3815.

Lechleiter, J., Hellmiss, R., Duerson, K., Ennulat, D., David, N., Clapham, D., and Peralta, E.G. (1990). Distinct sequence elements control the specificity of G protein activation by muscarinic acetylcholine receptor subtypes. EMBO J. *9*, 4381–4390.

Logothetis, D.E., Kurachi, Y., Galper, J., Neer, E.J., and Clapham, D.E. (1987). The βγ subunits of GTP-binding proteins activate the muscarinic K+ channel in heart. Nature *325*, 321–326.

Pfaffinger, P.J., Martin, J.M., Hunter, D.D., Nathanson, N.M., and Hille, B. (1985). GTP-binding proteins couple cardiac muscarinic receptors to a K channel. Nature *317*, 536–538.

Reuveny, E., Slesinger, P.A., Inglese, J., Morales, J.M., Iñiguez-Lluhi, J.A., Lefkowitz, R.J., Bourne, H.R., Jan, Y.N., and Jan, L.Y. (1994). Activation of the cloned muscarinic potassium channel by G protein βγ subunits. Nature *370*, 143–146.

Soejima, M., and Noma, A. (1984). Mode of regulation of the ACh-sensitive K-channel by the muscarinic receptor in rabbit atrial cells. Pflügers Arch. *400*, 424–431.

Tsukada, S., Simon, M.I., Witte, O.N., and Katz, A. (1994). Binding of βγ subunits of heterotrimeric G proteins to the PH domain of Bruton tyrosine kinase. Proc. Natl. Acad. Sci. USA *91*, 11256–11260.

Wei, A., Solaro, C., Lingle, C., and Salkoff, L. (1994). Calcium sensitivity of BK-type KCa channels determined by a separable domain. Neuron *13*, 671–681.

Wickman, K.D., Iñiguez-Lluhi, J.A., Davenport, P.A., Taussig, R., Krapivinsky, G.B., Linder, M.E., Gilman, A.G., and Clapham, D.E. (1994). Recombinant G-protein βγ-subunits activate the muscarinic-gated atrial potassium channel. Nature *368*, 255–257.